INTERNATIONAL JOURNAL FOR NUMERICAL METHODS IN FLUIDS, VOL. 20, 421–442 (1995)

WHY YOU SHOULD NOT USE 'HYBRID', 'POWER-LAW' OR RELATED EXPONENTIAL SCHEMES FOR CONVECTIVE MODELLING—THERE ARE MUCH BETTER ALTERNATIVES

B. P. LEONARD AND J. E. DRUMMOND

Center for Computational Mechanics, The University of Akron, Akron, OH 44325-3903, U.S.A.

SUMMARY

In many areas of computational fluid dynamics, especially numerical convective heat and mass transfer, the 'Hybrid' and 'Power-Law' schemes have been widely used for many years. The popularity of these methods for steady-state computations is based on a combination of algorithmic simplicity, fast convergence, and plausible looking results. By contrast, classical (second-order central) methods often involve convergence problems and may lead to obviously unphysical solutions exhibiting spurious numerical oscillations. Hybrid, Power-Law, and the exponential-difference scheme on which they are based give reasonably accurate solutions for steady, quasi-one-dimensional flow (when the grid is aligned with the main flow direction). However, they are often also used, out of context, for flows oblique or skew to the grid, in which case, inherent artificial viscosity (or diffusivity) seriously degrades the solution. This is particularly troublesome in the case of recirculating flows, sometimes leading to *qualitatively* incorrect results—since the effective artificial numerical Reynolds (or Péclet) number may then be orders of magnitude less than the correct physical value. This is demonstrated in the case of thermally driven flow in tall cavities, where experimentally observed recirculation cells are *not* predicted by the exponential-based schemes. Higher-order methods correctly predict the onset of recirculation cells. In the past, higher-order methods have not been popular because of convergence difficulties and a tendency to generate unphysical overshoots near (what should be) sharp, monotonic transitions. However, recent developments using robust deferred-correction solution methods and simple flux-limiter techniques have eliminated all of these difficulties. Highly accurate, physically correct solutions can now be obtained at optimum computational efficiency.

KEY WORDS: finite difference; finite volume; artificial viscosity; QUICK; hybrid; power-law

1. EXPONENTIAL-BASED SCHEMES

Exactly 40 years ago, Allen and Southwell[1] developed what is now called exponential differencing[2] for convection–diffusion operators. In the intervening period, several researchers have independently 'rediscovered' and/or approximated the basic elements of the Allen–Southwell scheme. The most notable of these convection–diffusion methods are the 'Hybrid' difference scheme of Spalding[3] and the 'Power-Law' difference scheme of Patankar.[4] These were combined with the SIMPLE pressure-solver[4] in the so-called TEACH code[5] developed at Imperial College, giving a robust, general-purpose elliptic-equation solver suitable for solving steady-state Navier–Stokes equations and associated heat and mass transfer problems. Over the past decade or more, the Hybrid and Power-Law methods have been used widely. Their popularity seems to have been increasing in recent years: at the most recent Thermal Problems conference[6] in

CCC 0271–2091/95/060421–22

Received 18 February 1994
Revised 2 November 1994

Swansea, fully half of the convection papers used the Power-Law scheme and an additional quarter used Hybrid.

In order to understand the basic properties of exponential-based schemes, consider the following idealized *steady, one-dimensional, constant-coefficient, source-free,* convection–diffusion problem for a scalar (such as temperature, for example)

$$u\frac{\mathrm{d}T}{\mathrm{d}x} = D\frac{\mathrm{d}^2T}{\mathrm{d}x^2} \tag{1}$$

where u is the convecting velocity and D is the diffusivity, with a downstream boundary condition

$$T(L) = 1 \tag{2}$$

and with

$$T(-\infty) = 0 \tag{3}$$

far upstream. The exact solution is

$$T(x) = \exp[-Pé(1 - x/L)] \tag{4}$$

where $Pé$ is the macroscopic Péclet number

$$Pé = \frac{uL}{D} \tag{5}$$

or Reynolds number in the case of momentum or vorticity transport (replace D by the kinematic viscosity, ν).

Now consider a second-order central-difference approximation of equation (1)

$$u\left(\frac{T_{i+1} - T_{i-1}}{2h}\right) = D\left(\frac{T_{i+1} - 2T_i + T_{i-1}}{h^2}\right) \tag{6}$$

using a uniform grid of mesh-width h. This can be rewritten as

$$(2 - P_\Delta)T_{i+1} - 4T_i + (2 + P_\Delta)T_{i-1} = 0 \tag{7}$$

introducing the grid Péclet number (or, equivalently, the cell Reynolds number)

$$P_\Delta = \frac{uh}{D} \tag{8}$$

Let k be an integer, defined for discrete values of x by

$$k = \left(1 - \frac{x}{L}\right)\frac{L}{h} \tag{9}$$

Then, for boundary conditions given by equations (2) and (3), the *difference* equation, (7), has an *exact* solution

$$T_k(\text{central}) = \left(\frac{2 - P_\Delta}{2 + P_\Delta}\right)^k \tag{10}$$

Note that this is oscillatory if $P_\Delta > 2$.

Using equation (9), the *exact* solution of the *differential* equation can be written, for discrete node values, as

$$T_k(\text{exact}) = (\mathrm{e}^{-P_\Delta})^k \tag{11}$$

For $P_\Delta < 2$, the argument in equation (10) is positive but less than the exponential argument of equation (11). The central-difference solution is similar in form to that of the exact continuous solution, but appears to be somewhat less diffusive. The basic idea behind the Allen–Southwell scheme is to *artificially decrease* the P_Δ in equation (10) so as to match the exact solution of the differential equation, (11). In other words, replace P_Δ in equation (10) by P_Δ^* (to be found) so that

$$\frac{2 - P_\Delta^*}{2 + P_\Delta^*} = e^{-P_\Delta} \tag{12}$$

giving an explicit formula for the artificial 'effective' grid Péclet number

$$P_\Delta^* = 2 \tanh(P_\Delta/2) = \mathscr{F}(P_\Delta) \tag{13}$$

Note that for small P_Δ,

$$P_\Delta^* \approx P_\Delta, \quad P_\Delta \text{ small} \tag{14}$$

and for large P_Δ,

$$P_\Delta^* \to 2, \quad P_\Delta \text{ large} \tag{15}$$

In fact, $P_\Delta^* \approx 2$ for P_Δ above about 6. This is seen in Figure 1.

Figure 1 also shows three approximations to the hyperbolic tangent function. The piecewise-linear approximation is equivalent to the Hybrid scheme

$$\begin{aligned} &P_\Delta^*(\text{Hybrid}) = P_\Delta \quad \text{for } 0 \leqslant P_\Delta \leqslant 2 \\ &P_\Delta^*(\text{Hybrid}) \equiv 2 \quad \text{for } P_\Delta \leqslant 2 \end{aligned} \tag{16}$$

The triangles show the Power-Law approximation

$$\begin{aligned} &P_\Delta^*(\text{Power-Law}) = \frac{2P_\Delta}{P_\Delta + 2(1 - 0{\cdot}1\, P_\Delta)^5} \quad \text{for } 0 \leqslant P \leqslant 10 \\ &P_\Delta^*(\text{Power-Law}) \equiv 2 \quad \text{for } P \geqslant 10 \end{aligned} \tag{17}$$

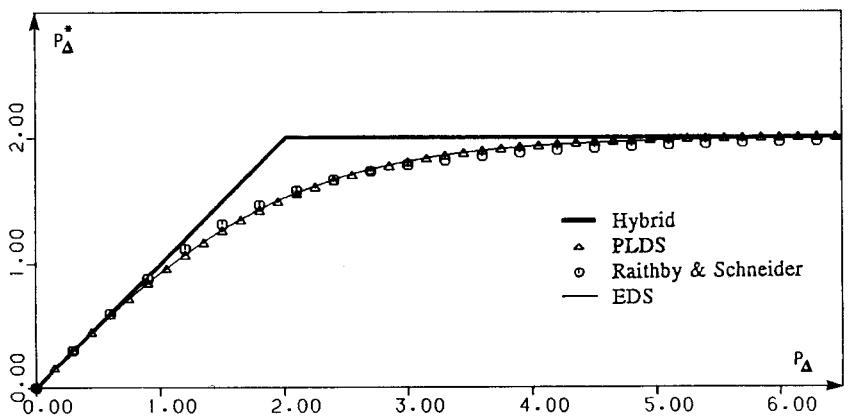

Figure 1. Effective grid Péclet number for EDS and various approximations

and the circles show the algebraic approximation of Raithby and Schneider[2]

$$P_\Delta^*(\text{R\&S}) = \left[\frac{P_\Delta^2}{2(5+P_\Delta^2)} + \frac{(1+0{\cdot}005\,P_\Delta^2)}{P_\Delta(1+0{\cdot}05\,P_\Delta^2)}\right]^{-1} \tag{18}$$

The exponential scheme, equation (13), and the above approximations are based on using second-order central differencing for both convection and diffusion, but with an *artificially enhanced* diffusion coefficient

$$D^* = D + D_{\text{art}} = \frac{uh}{P_\Delta^*} \tag{19}$$

The *additional* artificial diffusivity is thus given by

$$\frac{D_{\text{art}}}{D} = \frac{P_\Delta}{2}\coth\left(\frac{P_\Delta}{2}\right) - 1 \tag{20}$$

Note, from equation (19), that when $P_\Delta^* = 2$, the total effective diffusivity is

$$D^*(P_\Delta^* = 2) = \frac{uh}{2} \tag{21}$$

This is the effective artificial numerical diffusivity inherent in first-order upwinding for convection.[7] In other words, for the exponential convection–diffusion scheme (and the various approximations thereof), when $P_\Delta^* \to 2$, the scheme is equivalent to using

first-order upwinding for convection
with physical diffusion terms ignored.

Note that for the Hybrid approximation, this occurs when the physical grid Péclet number, P_Δ, is above 2. For the exponential scheme itself (and the Power-Law and algebraic approximations) this occurs for P_Δ values above about 6. For the one-dimensional model problem on which exponential-difference schemes are based, this is an appropriate approximation: using first-order convection and neglecting (streamwise) diffusion gives the result that the scalar is swept downstream unchanged. First-order upwinding does not 'recognise' the downstream boundary condition—which therefore has no effect on the solution.

In two-dimensional flows, exponential-differencing (or one of its approximations) is used componentwise; i.e. the convection–diffusion flux in each component direction is based on an effective local *component* grid Péclet number; for example

$$P_{\Delta x}^* = \left(\frac{u\,\Delta x}{D_x}\right) = \mathscr{F}(P_{\Delta x}) \tag{22}$$

and

$$P_{\Delta y}^* = \left(\frac{v\,\Delta y}{D_y}\right) = \mathscr{F}(P_{\Delta y}) \tag{23}$$

In two dimensions, the schemes work best when one of the physical component grid Péclet numbers is very small. For example, $P_{\Delta y}$ might be small because of small v values (the main flow direction is approximately aligned with the x axis), or Δy is small (fine mesh in the transverse direction), or D_y is large (large physical transverse diffusivity). In three dimensions, two of the physical component grid Péclet numbers need to be small. These are quasi-one-dimensional

flows, with the main flow direction aligned with a grid co-ordinate. However, in many flows of practical interest, the flow direction may be oblique or skew to the grid. In such cases, component grid Péclet numbers may be large in more than one direction. This introduces large amounts of 'cross-wind' artificial diffusion, as discussed in Section 2.

2. ARTIFICIAL NUMERICAL DIFFUSION

Problems arise when the very strict conditions on which the exponential difference schemes (EDS) are based are relaxed. The EDS-based schemes work well for steady, quasi-one-dimensional flow (e.g. axial convection with transverse diffusion, such as occurs in boundary-layer and pipe flow)—provided the convecting velocity is (very nearly) aligned with one of the grid co-ordinates. To be more precise, the EDS model-problem conditions are listed here again:

(i) steady-state conditions,
(ii) one-dimensionality,
(iii) constant coefficients,
(iv) source free.

To the extent that the flow conditions closely approximate these requirements, EDS-based schemes give tolerable results. Conversely, if any of these conditions is seriously violated, one should expect corresponding degradation of the solution.

2.1. Unsteady flow

Under most conditions of practical interest, the component grid Péclet number in the main flow direction is likely to be much larger than 1. This means that EDS-based schemes are operating as first-order upwinding for convection with physical diffusion neglected. As is well known,[7] first-order upwinding is extremely artificially diffusive for transient problems. This is seen in Figure 2, where distinct initial profiles under (what should be) purely convective conditions are soon erroneously converted into spreading Gaussian-like blobs. For this reason, EDS-based schemes are not usually used for unsteady flow calculations.

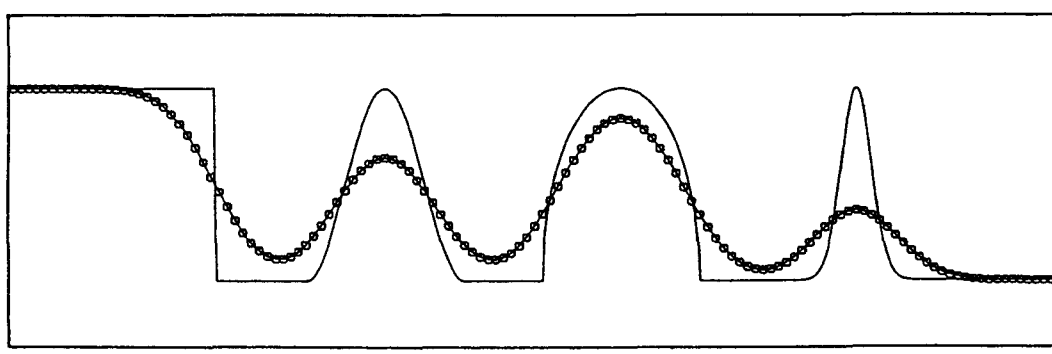

Figure 2. Artificial diffusion of first-order upwinding in transient problems. Purely convective flow from left to right

2.2. *Multidimensions*

By far the most serious *misapplication* of EDS-based schemes, such as Hybrid and Power-Law, is to multidimensional problems involving high-speed flow oblique or skew to the grid mesh. In this case, more than one component grid Péclet number is large at any given control volume cell. This means that the scheme is equivalent to first-order upwinding for convection with physical diffusion neglected. This gives rise to serious cross-wind artificial diffusion, as sketched in Figure 3. Part (a) of the figure shows the true physical situation: large component velocities together with small component diffusive fluxes, giving rise to a large oblique convecting velocity and small transverse (cross-wind) as well as small streamwise diffusion. Part (b) of the figure suggests enhanced componentwise artificial diffusion (of magnitude $u\,\Delta x/2$ in the x-direction and $v\,\Delta y/2$ in the y-direction). This means that the effective diffusive flux is artificially higher in *all* directions. The larger streamwise component diffusion is not so much of a problem, since the convection term is still dominant (after all, this is what happens in quasi-one-dimensional flows). However, the artificially enhanced cross-wind diffusive flux can have devastating effects—e.g. a sharp jump in value across the transverse direction (a shear layer or a discontinuity in temperature or species concentration) will be artificially smeared far beyond what should occur physically.

There is another subtlety that should be stressed. Most flows of practical interest are turbulent, and the flow solver typically couples continuity, scalar transport, and momentum equations (plus pressure-solver) with sophisticated (and expensive!) multi-equation turbulence models. The turbulence equations predict the physical turbulent diffusivity (viscosity) on which the component grid Péclet (Reynolds) numbers are based. If these exceed 2 in the case of Hybrid or about 6 for Power-Law (or EDS itself), the expensively calculated physical diffusivity (viscosity) is

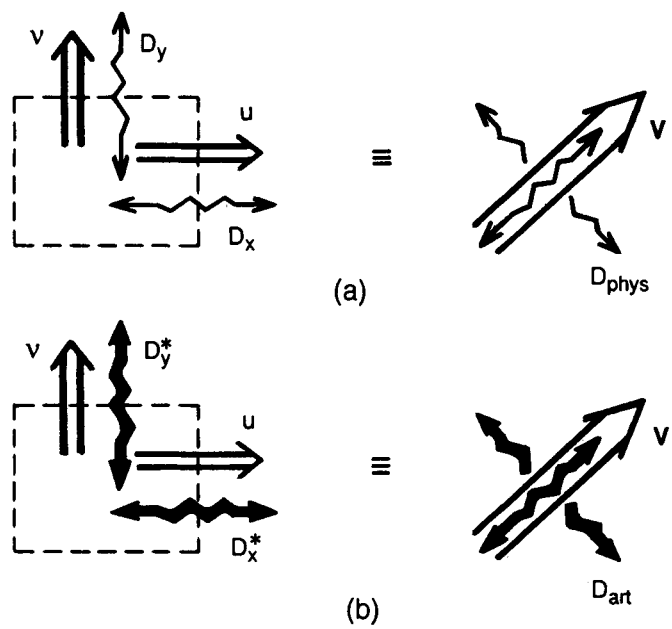

Figure 3. Schematic of cross-wind artificial diffusion. (a) Physical situation. (b) Using EDS-based method

ignored—and replaced by $u\,\Delta x/2$ and $v\,\Delta y/2$, componentwise. This means that the resulting predicted flow is *largely insensitive to the turbulence model used* (except where the stream direction happens to coincide with a grid direction).

2.3. *Smith–Hutton test problem*

The artificial diffusion of EDS-based schemes used for multidimensional transport is easily demonstrated by using a scalar test problem such as that devised by Smith and Hutton.[8] Figure 4 shows the prescribed velocity profile given by

$$u = 2y(1 - x^2) \tag{24}$$

$$v = -2x(1 - y^2) \tag{25}$$

and an inlet temperature profile

$$T_{\text{in}}(x) = 1 + \tanh[\alpha(1 + 2x)] \tag{26}$$

where α is a steepness parameter, taken, in this case, to be 100. The steady transport equation to be solved is

$$\mathbf{v} \cdot \nabla T = \frac{1}{Pe} \nabla^2 T \tag{27}$$

for the case of a constant Péclet number, $Pe = 500$.

Figure 5 shows results, in terms of the predicted outlet profile, using the Power-Law scheme on three different grid meshes, 20×10, 40×20, and 80×40. The reference solution is obtained by using a very high-order method on a very fine (160×80) grid.[9] The artificially diffusive nature of the EDS-based scheme is clearly evident. Also note the very slow convergence as the mesh is

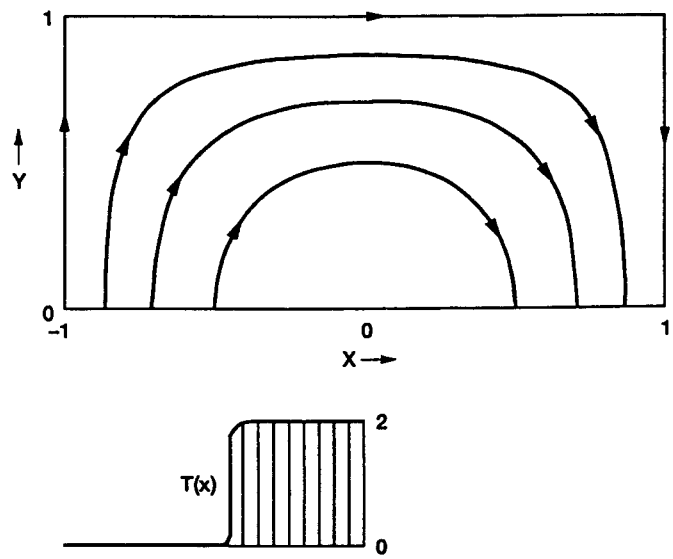

Figure 4. Velocity field and inlet profile for the Smith–Hutton problem

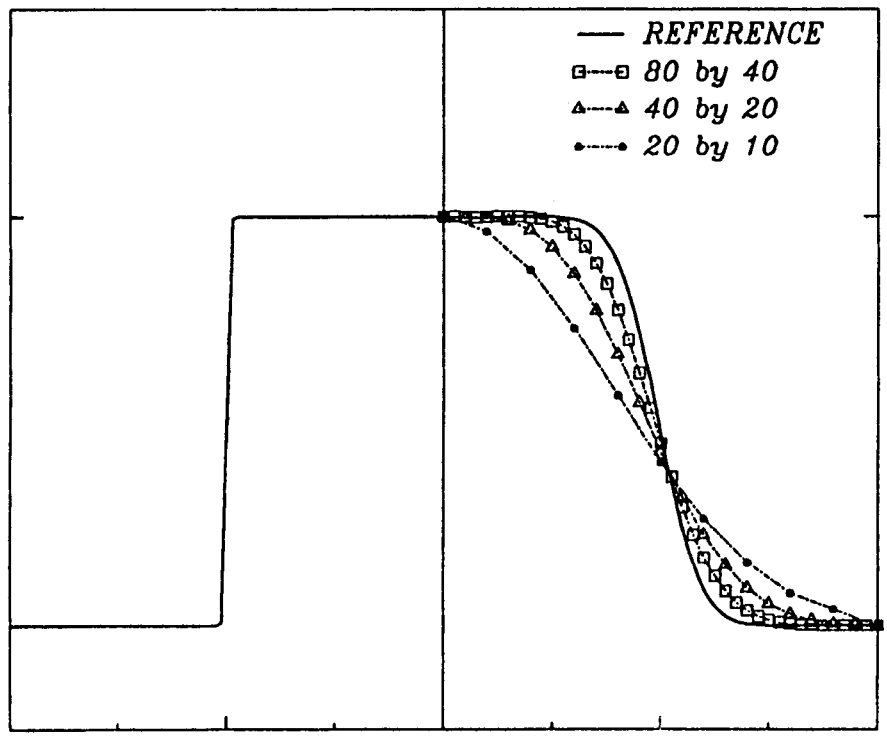

Figure 5. Outlet profile for the Power-Law solution of the Smith–Hutton problem

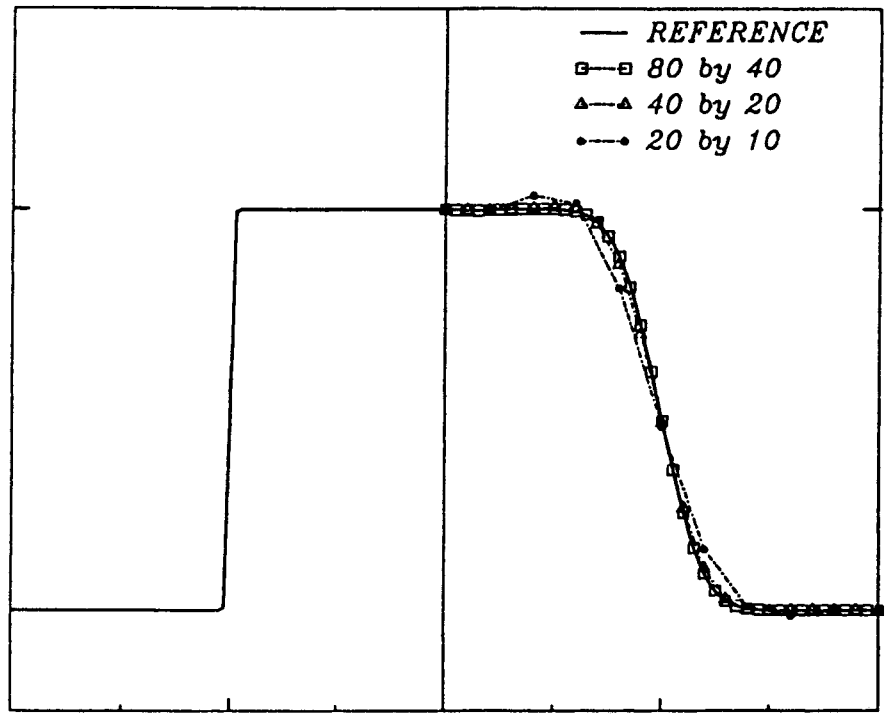

Figure 6. Outlet profiles using the QUICK-2D scheme

refined. By contrast, Figure 6 shows results of the same test problem using the two-dimensional QUICK scheme[10] (third-order upwind-weighted convection, second-order diffusion). Although the coarse-mesh solution shows a little numerical smearing and a small overshoot, the solution is essentially converged at the 40×20 refinement. Accurate and efficient solutions of this kind are easy to obtain;[9] a simple flux-limiter technique for eliminating potential overshoots near rapid transition regions is outlined below, and has been discussed in detail elsewhere.[11]

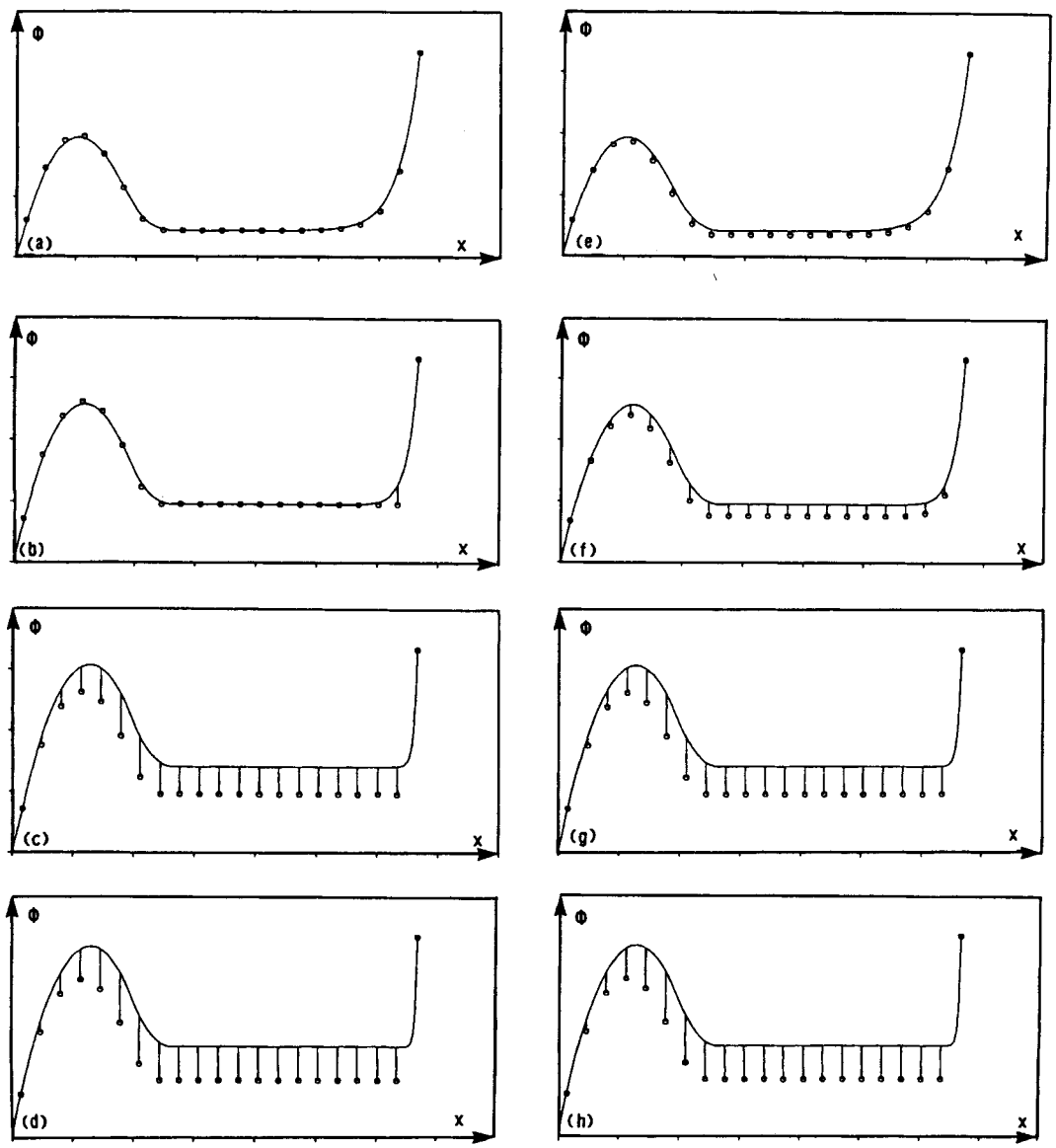

Figure 7. Source-term test problem using Hybrid (left) and Power-Law (right). (a), (e): $P_\Delta = 1$; (b), (f): $P_\Delta = 2$; (c), (g): $P_\Delta = 6$; (d), (h): $P_\Delta = 10$

2.4 Variable coefficients

Provided the flow is steady, essentially quasi-one-dimensional (with the main flow aligned with a grid coordinate), and relatively source-free, EDS-based schemes seem to be insensitive to relaxing the constant-coefficient condition. This is easy to understand because the problem can be broken up into a series of little one-dimensional convection–diffusion problems across control volumes, each one amounting to a two-point boundary-value problem using the *local* values of u and D. In each case, an exponential solution is appropriate, although the length-constant changes from point to point along the mesh. This is the most useful setting for EDS-based schemes. It should be noted, however, that higher-order, flux-limited methods generally give even more accurate solutions under these conditions.

2.5. Source terms

Even when the flow is steady and one-dimensional, source terms, such as pressure-gradients or mass or energy sources (or sinks), can cause serious problems for EDS-based schemes. This has been discussed elsewhere.[11] using a simple test problem with a known exact solution. Figure 7, taken from Reference 11, shows results for Hybrid calculations (on the left) and Power-Law results (on the right) for grid Péclet numbers of 1, 2, 6, and 10. For $P_\Delta = 1$ and 2, Hybrid is operating as second-order central for both convection and diffusion, and gives reasonable results. Above $P_\Delta = 2$, the numerical solution saturates (physical diffusion is omitted and replaced by artificial numerical diffusion, $u\,\Delta x/2$); artificial diffusion in the presence of source terms is seen to produce significant error.[12] In the case of the Power-Law scheme, errors are noticeable even at the lower P_Δ values. Note that saturation occurs, in this case, at around $P_\Delta \sim 6$, in conformance with Figure 1.

3. NATURAL CONVECTION IN TALL CAVITIES

Two-dimensional, buoyancy-driven flow in a tall, rectangular cavity shows one of the possible effects of using the diffusive EDS-based schemes. Figure 8 shows the geometry of such an

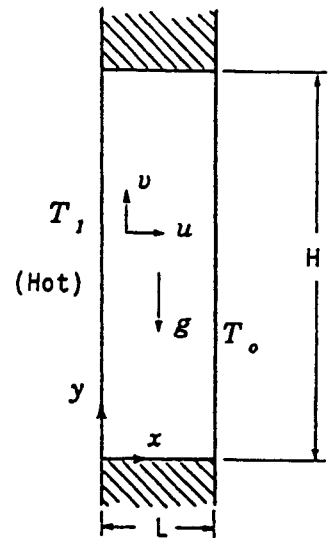

Figure 8. Geometry of the tall cavity

enclosure which is bounded by two vertical, isothermal walls of differing temperature and two horizontal walls that are insulated. The flow is driven as the fluid is heated at the hot wall. It then rises and turns at the top of the cavity and falls along the cold wall as it gives up heat. The basic unicellular flow can give way to multicellular flow for certain flow parameters, as reported by Vest and Arpaci.[13]

The governing equations may be cast in vorticity–stream-function variables and non-dimensionalized by scaling the velocities by $U = \gamma g L^2 \Delta T/\nu$, where γ is the coefficient of volumetric expansion, g the gravitational field, ν the kinematic viscosity, and ΔT the temperature difference between the two vertical walls. The cavity dimensions are scaled by L, the time by L^2/ν, and the temperatures are calculated with respect to the cold wall and scaled with ΔT. The vorticity, ω, and stream-function, ψ, are scaled with U/L and UL, respectively. This non-dimensionalization was previously used by Drummond and Korpela.[14] Applying the standard Boussinesq approximation[7] gives the following forms of the vorticity transport, energy and Poisson equations:

$$\frac{\partial \omega}{\partial t} + Gr\left[\frac{\partial (u\omega)}{\partial x} + \frac{\partial (v\omega)}{\partial y}\right] = \left[\frac{\partial^2 \omega}{\partial x^2} + \frac{\partial^2 \omega}{\partial y^2}\right] + \frac{\partial T}{\partial x} \tag{28}$$

$$\frac{\partial T}{\partial t} + Gr\left[\frac{\partial (uT)}{\partial x} + \frac{\partial (vT)}{\partial y}\right] = \frac{1}{Pr}\left[\frac{\partial^2 T}{\partial x^2} + \frac{\partial^2 T}{\partial y^2}\right] \tag{29}$$

$$\frac{\partial^2 \psi}{\partial x^2} + \frac{\partial^2 \psi}{\partial y^2} = -\omega \tag{30}$$

The vorticity and stream-function are defined by

$$\omega = \frac{\partial v}{\partial x} - \frac{\partial u}{\partial y} \tag{31}$$

$$u = \frac{\partial \psi}{\partial y}, \quad v = -\frac{\partial \psi}{\partial x} \tag{32}$$

The Grashof number is defined as $Gr = UL/\nu$, while the Prandtl number is $Pr = \nu/\alpha$, where α is the thermal diffusivity. The velocity components u and v correspond to the co-ordinates x and y, respectively, and T is the dimensionless temperature. The enclosure can be scaled to a dimensionless height of $A = H/L$, where A is the aspect ratio, and a width of 1·0. The boundary conditions are as follows:

$$\begin{aligned}
&u = \frac{\partial \psi}{\partial y} = 0 \quad @\ y = 0, A \\
&v = \frac{\partial \psi}{\partial x} = 0 \quad @\ x = 0, 1 \\
&\psi = 0 \quad @\ y = 0, A; \quad x = 0, 1 \\
&T_1 = 1 \text{ (left wall)}, \quad T_0 = 0 \text{ (right wall)} \\
&\frac{\partial T}{\partial y} = 0 \quad @\ y = 0, A \text{ (bottom, top walls)}
\end{aligned} \tag{33}$$

As described in detail in the work of Drummond *et al.*,[15] the numerical solution of the equations is obtained using schemes based on QUICK, Hybrid differencing, Power-Law differencing, first-order upwinding and the artificial-diffusion-free method of Arakawa.[16] Solutions are

achieved by explicit time-marching to the steady-state solution. For the problem with $A = 33{\cdot}0$, $Gr = 9500$ and $Pr = 0{\cdot}71$, the resulting flow patterns are shown in Figure 9. A 31×129 grid having uniform spacing in the x- and y-directions was used. Note that secondary circulations are present with the QUICK and Arakawa calculations, but suppressed by the other schemes. This result is not unexpected since values of P_Δ are greater than 10 over much of the flow field. It is of interest that the cells shown in the figure were observed experimentally by Vest and Arpaci[13] and that the cell spacings predicted using the QUICK and Arakawa schemes were within 3 per cent of that found in the experimental study.

The damping of the secondary flows is also evident when looking at the maximum vorticity in the core of the cavity, a reasonable indicator of the onset of cell formation. For a cavity with $A = 10{\cdot}0$ and a highly conductive fluid with Pr close to zero, Figure 10 shows the variation of the maximum core vorticity versus Grashof number. A sharp increase in vorticity is displayed by the QUICK and Arakawa calculations as cells start to form near $Gr = 8000$, a value very close to the critical Grashof number typical of low-Pr flows. On the other hand, the Hybrid and Power-Law calculations show a much more gradual rise that indicates a damping of the onset of secondary cells. Interestingly, the purportedly more accurate Power-Law scheme shows virtually the same results as Hybrid. First-order upwinding is obviously the most diffusive.

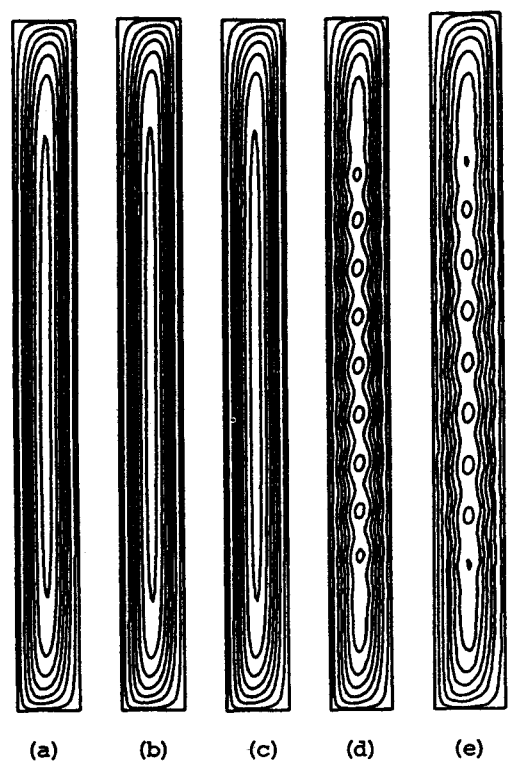

Figure 9. Streamline patterns: (a) First-order upwind; (b) Hybrid; (c) Power-Law; (d) Arakawa; (e) QUICK

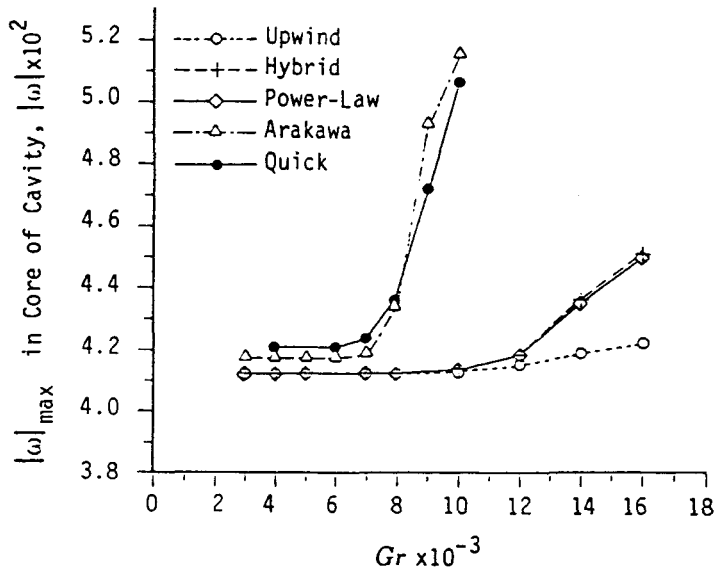

Figure 10. Maximum magnitude of vorticity in the core of the cavity

4. HIGHER-ORDER CONVECTION

The main motivating factor behind the development and subsequent popularity of EDS-based schemes seems to be the fact that they have *fast convergence* properties (when used in iterative solution procedures) and that they generate *non-oscillatory* results. Both of these features are related to the feedback stability properties of the convection–diffusion operator. In the case of central-differencing methods (of any order), there is no convective feedback sensitivity,[10] so that under high-convection conditions (large *Pé*), stability problems and numerical oscillations are likely to occur. To see this, consider the unsteady convection–diffusion equation for a node value

$$\frac{\partial T_i}{\partial t} = \left[-\frac{\partial T}{\partial x} + \frac{1}{P_\Delta}\frac{\partial^2 T}{\partial x^2} \right]_{\text{model}} = [\text{RHS}]_{\text{model}} \tag{34}$$

where the time-derivative can also represent an iterative term in a steady-state calculation, and the non-dimensionalization is based on the mesh size (i.e. $h = 1$). The evolution of a perturbation in T_i can be studied by writing

$$\frac{\partial \delta T_i}{\partial t} = \frac{\partial [\text{RHS}]_{\text{model}}}{\partial T_i}\,\delta T_i \tag{35}$$

which has a formal solution

$$\delta T_i = \exp(\Sigma t) \tag{36}$$

where Σ is the feedback sensitivity

$$\Sigma = \frac{\partial [\text{RHS}]_{\text{model}}}{\partial T_i} \tag{37}$$

For numerical perturbations to die out rapidly, Σ needs to be negative and of substantial magnitude. Also, in an iterative matrix solution of the steady-state equation,

$$[\mathrm{RHS}]_{\mathrm{model}} = 0 \tag{38}$$

desirable diagonal dominance conditions correspond to large absolute values of Σ.

Now consider the second-order central-difference model of equation (34)

$$[\mathrm{RHS}]_{\mathrm{model}} = -\frac{1}{2}(T_{i+1} - T_{i-1}) + \frac{1}{P_\Delta}(T_{i+1} - 2T_i + T_{i-1}) \tag{39}$$

In this case,

$$\Sigma_{2C} = -\frac{2}{P_\Delta} \tag{40}$$

Note that there is *no contribution from the convection term.* Under the high grid Péclet (Reynolds) numbers of practical calculations, second-order-central feedback sensitivity is extremely weak. For the same reason, the matrix structure is diagonally submissive, and iterative solutions are not straightforward.

By contrast, the feedback sensitivity of the exponential-difference scheme is

$$\Sigma_{\mathrm{EDS}} = -\frac{2}{P_\Delta^*} = -\coth(P_\Delta/2) \tag{41}$$

Under high-convection conditions, this approaches -1, representing the strong negative feedback sensitivity of first-order upwinding for convection. The matrix structure is diagonally dominant, for the same reason. Any numerical perturbations are quickly damped out; whereas, in the central-difference case, parasitic oscillations may occur, and the algorithm has no way of sensing or responding to their growth.

Higher-order upwind-weighted convection methods have good feedback stability properties. For example, in one dimension, a family of control-volume methods can be constructed by writing the convection term as the difference of face values across a cell

$$-(T_r - T_l) \tag{42}$$

where (for positive convecting velocities)

$$T_r(i) = \tfrac{1}{2}(T_{i+1} + T_i) - CF\cdot(T_{i+1} - 2T_i + T_{i-1}) \tag{43}$$

and

$$T_l(i) = T_r(i-1) \tag{44}$$

and CF is a 'curvature factor'. For example for second-order upwinding[7]

$$CF = \tfrac{1}{2} \tag{45}$$

For (the steady-state form of) Fromm's method,[17]

$$CF = \tfrac{1}{4} \tag{46}$$

and for QUICK[18]

$$CF = \tfrac{1}{8} \tag{47}$$

The overall (convective-plus-diffusive) feedback sensitivity is then

$$\Sigma_{CF} = -3\,CF - \frac{2}{P_\Delta} \tag{48}$$

which is quite strongly negative, even under highly convective conditions.

4.1. *Deferred correction*

Higher-order upwind-weighted methods are potentially quite stable. But because of the wider stencil involved, one needs to be very careful when applying traditional *tridiagonal* matrix-solver techniques; simply casting outlying values into the source term can evidently lead to convergence problems. A much more stable iterative technique is based on the deferred-correction method.[19] This has recently been put on a very firm basis for a consistent iterative formulation using QUICK.[20] In an iterative calculation, one simply writes the 'new' face value in terms of the first-order-upwind face value plus a correction term. The first-order face value involves one or the other of the adjacent node values (depending on the local convecting velocity direction); the correction term is deferred (or lagged) from the previous 'old' values and lumped into the source term. More specifically, the face value is written

$$T_f = T_f^{(1st)}(\mathrm{TBC}) + \Delta T_f(\mathrm{OLD}) \tag{49}$$

where TBC stands for to-be-computed, and

$$\Delta T_f(\mathrm{OLD}) = T_f^{\mathrm{H.O.}}(\mathrm{OLD}) - T_f^{(1st)}(\mathrm{OLD}) \tag{50}$$

Clearly, as the steady-state solution is reached, the first-order contributions cancel, and the solution is consistent with using the higher-order face values everywhere. Iterative convergence is very fast.[20] Since a *tridiagonal* matrix structure is maintained, well-known codes (such as TEACH, for example) can easily be modified, simply by adding appropriate $\Delta T_f(\mathrm{OLD})$ terms to the source term at each grid point.[20]

4.2. *Flux limiters*

As is by now well known, higher-order upwind methods (in their basic form) suffer from 'overshoot' problems. Typically, a step-like profile which should be sharp and monotonic will be computed with an overshoot on one side or the other, or both. This was seen in Figure 6, for example. In many cases, the effect is small and can be ignored. However, there are situations in which the phenomenon can lead to non-linear instability. This might happen, for example, when a computed turbulence quantity overshoots a transition to small values and becomes (unphysically) negative (sometimes called an undershoot). If this were to result in a negative turbulent viscosity (or diffusivity), computational divergence would follow quickly. This has led some researchers to a strategy of using higher-order (usually QUICK) methods for the continuity, momentum, and energy equations, but Hybrid or Power-Law for the turbulence equations. Justification of this strategy has been based on the *assumption* that source terms dominate in the turbulence equations[21] (i.e. that convection and diffusion are not important).

Before 1988, modellers of highly convective flows had a choice between stable and non-oscillatory (essentially first-order) methods such as Hybrid or Power-Law, giving plausible (albeit highly artificially diffusive) results, on the one hand, and higher-order methods exhibiting clearly unphysical oscillations and convergence problems, on the other. Not surprisingly, most users

chose the former; and this is a habit continued today. But 1988 was a land-mark year for highly convective flow simulation. In that year, Gaskell and Lau[22] introduced their Sharp Monotonic Algorithm for Realistic Transport (SMART), and this was followed by Leonard's[23] Simple High-Accuracy Resolution Program (SHARP). These are flux-limiter strategies, similar in many respects to the 'TVD' schemes (described by Sweby,[24] for example) used in gasdynamic codes. In general terms, flux limiters guarantee that, in a steady-state finite-volume formulation, the convected face value, initially estimated on the basis of a high-order approximation, is constrained to lie within specified limits (described below). This eliminates extraneous overshoots (or undershoots) while still allowing high-order resolution of sharply varying features. First-order upwinding automatically satisfies the limiter constraints; but inherent artificial diffusion numerically smears initially sharp features.

4.3. ULTRA-SHARP strategy

A non-oscillatory strategy, based on the universal limiter for tight resolution and accuracy (ULTRA), has been described in detail elsewhere.[9,11] The ULTRA-SHARP strategy includes all other steady-state flux-limiter and TVD schemes as special cases. The main ideas are repeated here for convenience. Consider the finite-volume face shown in Figure 11, and define a *normalized variable* (such as temperature, for example) in the vicinity of the face as

$$\tilde{T}(x, y, z) = \frac{T(x, y, z) - T_U}{T_D - T_U} \tag{51}$$

Note, in Figure 11, that the definition of upwind (U), downwind (D), and central (C) nodes depends on the sign of the normal component of the convecting velocity at the face, u_n. Under locally monotonic conditions (T_C between T_U and T_D), the estimated face value, T_f, should be between T_C and T_D. In terms of normalized variables, this gives a necessary inequality

$$\tilde{T}_C \leqslant \tilde{T}_f \leqslant 1 \quad \text{for } 0 \leqslant \tilde{T}_C \leqslant 1 \tag{52}$$

This, however, is not sufficient to guarantee non-oscillatory behaviour (e.g. second-order central differencing satisfies this condition). An important additional condition requires $\tilde{T}_f$ to vanish with $\tilde{T}_C$; i.e.

$$\tilde{T}_f \to 0 \quad \text{as } \tilde{T}_C \to 0_+ \tag{53}$$

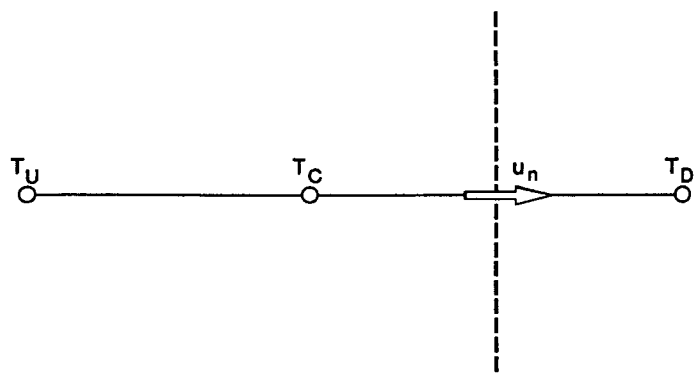

Figure 11. Definition of local node values based on the sign of u_n

Under locally non-monotonic conditions, various strategies are possible. One of the simplest is to choose

$$\tilde{T}_f = \tilde{T}_C \quad \text{for } \tilde{T}_C < 0 \text{ or } \tilde{T}_C > 1 \tag{54}$$

Other relationships providing continuity at ($\tilde{T}_C = \tilde{T}_f = 0$) and ($\tilde{T}_C = \tilde{T}_f = 1$) have been used; e.g. in Reference 11,

$$\tilde{T}_f = \tfrac{3}{2}\tilde{T}_C \quad \text{for } \tilde{T}_C < 0 \tag{55}$$

and

$$\tilde{T}_f = \tfrac{1}{2} + \tfrac{1}{2}\tilde{T}_C \quad \text{for } \tilde{T}_C > 1 \tag{56}$$

The universal limiter constraints can be summarized in the *normalized variable diagram*—a plot of the normalized face value, $\tilde{T}_f$, against the normalized adjacent upstream value, $\tilde{T}_C$. This is shown in Figure 12, using equation (54) in the non-monotonic regions. The additional constraint boundary, OB,

$$\tilde{T}_f = \text{const} \times \tilde{T}_C \tag{57}$$

is added near $\tilde{T}_C \to 0_+$ in order to avoid indeterminacy. The slope constant should be chosen to be fairly large, say $O(10)$, so as to maintain sharp resolution. It should be mentioned that TVD schemes use a slope of 2 for this constraint; this introduces smearing of (what should be) sharp profiles.

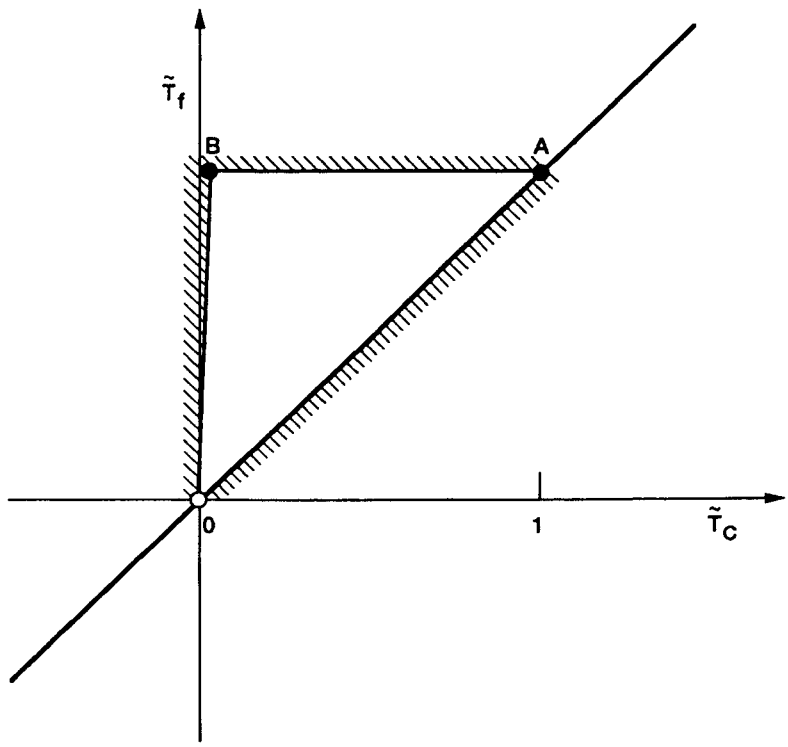

Figure 12. Normalized variable diagram showing the universal limiter constraints

In general terms, the ULTRA-SHARP strategy proceeds as follows. (i) Compute a tentative high-order (multidimensional) face value, T_f. (ii) Normalize this and the corresponding T_C. (iii) If the point $(\tilde{T}_C, \tilde{T}_f)$ lies within the triangular region OAB in Figure 12, use the face value without modification. (iv) Otherwise, take the nearest constraint boundary at the same $\tilde{T}_C$ value (reconstructing the corresponding unnormalized face value). In practice, there is no need to use normalized variables at all. Instead, successive application of the 'median' function[25] results in a straightforward, inexpensive (and vectorizable) algorithm. The median function of three numbers a, b and c,

$$f = \text{MED}(a, b, c) \tag{58}$$

selects the number that lies between the other two. This is easily implemented using combinations of standard (e.g. FORTRAN) functions.[25] For the universal limiter, define three (unnormalized) reference quantities

$$T_1 = T_C \tag{59}$$

$$T_2 = T_D \tag{60}$$

and, following equation (57),

$$T_3 = T_U + \text{const} \times (T_C - T_U) \tag{61}$$

These correspond to (indefinite extensions of) lines OA, BA, and OB, respectively, in Figure 12. Now define

$$T_4 = \text{MED}(T_1, T_2, T_3) \tag{62}$$

After computing a tentative higher-order face value, $T_f^{H.O.}$, the face value actually used is then

$$T_f = \text{MED}(T_1, T_4, T_f^{H.O.}) \tag{63}$$

This is the exact equivalent of Figure 12. In an iterative calculation, use of the deferred correction technique then leads to very fast convergence, giving highly accurate, *non-oscillatory* results.

To see the effect of using ULTRA-SHARP, Figure 13 shows the results of using ULTRA-QUICK for the convection terms in the Smith–Hutton problem previously considered; second-order central differencing is used for the (small) diffusion terms. By comparison with Figure 6, one sees that the coarse-grid overshoot has been eliminated without smearing the profile. In this case, the (effectively) third-order ULTRA-QUICK scheme is not quite able to adequately resolve the steep transition region on the coarse 20×10 mesh. However, the ULTRA-SHARP strategy can be used with (in principle, arbitrarily) high-order convection schemes. Figure 14 shows ULTRA-SHARP results for a variable-order convection scheme,[9] again using second-order diffusion terms. In this case, $T_f^{H.O.}$ in equation (63) is based on the third-order QUICK scheme in 'smooth' regions (identified by low values of normal gradient or change in gradient across a cell face); near sharply varying features, the algorithm automatically extends to a fifth- or seventh-order estimate of $T_f^{H.O.}$, using an appropriately expanded stencil. This is a cost-effective strategy, since the very high-order computations occur only at a relatively small fraction of grid points; however, the overall accuracy is greatly enhanced.

Of course, the higher-order ULTRA-SHARP convective computation is more expensive—*per grid point*—than a typical Hybrid or Power-Law calculation. But in a practical problem (involving a pressure solver—often the most expensive component—and several auxiliary variables), the overall cost increase is minimal (perhaps 15 or 20 per cent). However, the accuracy is increased dramatically—compare Figures 5 and 14. Stated another way: to achieve the accuracy indicated in Figure 14 using an EDS-based scheme would require such a prohibitively fine grid that the overall cost would be orders of magnitude larger.[9,11,22,26]

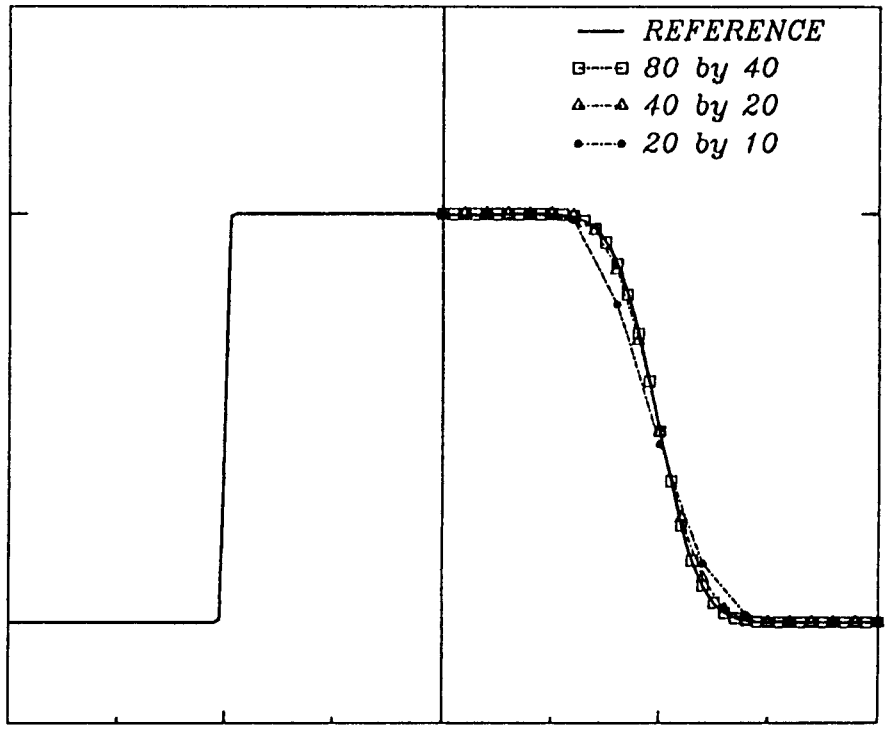

Figure 13. ULTRA-QUICK results for the Smith–Hutton problem

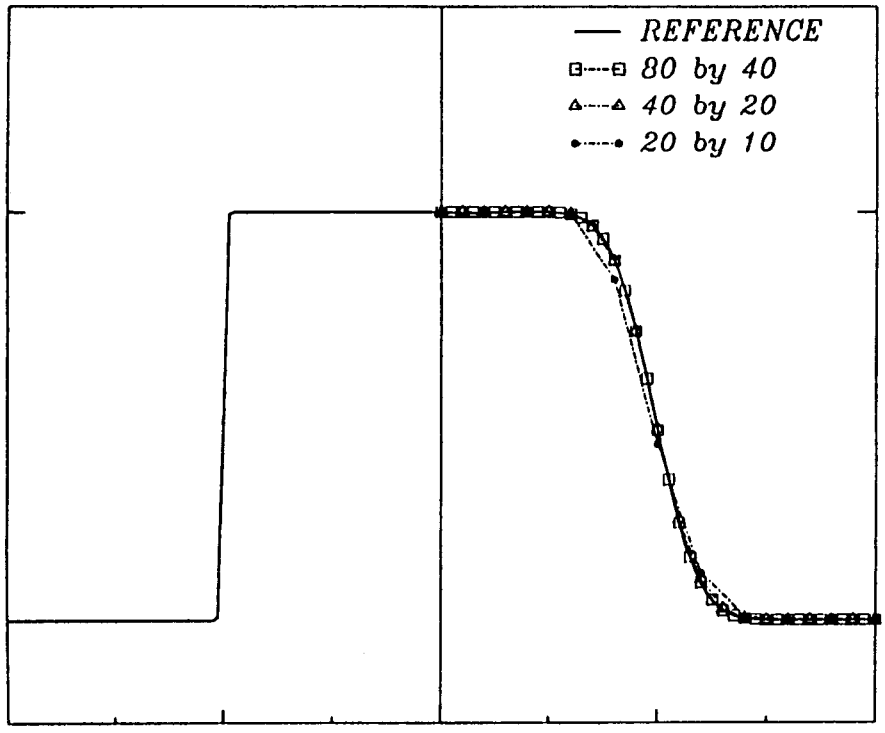

Figure 14. ULTRA-SHARP (3/5/7) results for the Smith–Hutton problem

5. CONCLUSION

This paper has attempted to demonstrate why the immensely popular Hybrid and Power-Law schemes (and related EDS-based methods) should *not* be used for practical CFD calculations—especially for convective modelling of heat and mass transfer processes. There are undoubtedly many EDS-based computations giving adequate agreement with experiment (or other benchmark numerical or analytical results). These schemes work best, for example, for steady-quasi-one-dimensional flow, where the main flow direction is (very nearly) aligned with a grid co-ordinate, and source terms are not strong. In this case, first-order upwinding for convection with physical diffusion neglected (but replaced by artificial diffusion) is being used in the main flow direction; *transverse* convective-plus-diffusive transport is then being adequately modelled by essentially second-order methods. In *some* cases involving flow oblique or skew to the grid, EDS-based schemes may give acceptable results. In most cases, these will be found to be flows dominated by the kinematic constraint of the (constant-density) continuity equation: that the velocity field should be solenoidal. Gradients (of velocity or scalar quantities) are then generally small—except in near-wall regions (where special 'wall-functions' are typically used,[4] and the flow is aligned with the grid). This is the classical potential-flow-plus-boundary-layer situation in which convection–diffusion processes are important only in the boundary-layer regions—where the flow is (very nearly) aligned with one of the grid co-ordinates.

When convection–diffusion processes are important throughout major regions of the flow field, EDS-based schemes break down for flows oblique or skew to the grid. This is because, for practical grid sizes, component grid Péclet or Reynolds numbers are typically much greater than the critical values of 2 (for Hybrid) or about 6 (for Power-Law and EDS itself), and the scheme is operating as first-order upwinding for convection with physical diffusion ignored (and replaced by artificial diffusion equivalent to setting *all* component grid Péclet or Reynolds numbers equal to 2). Three points should be noted.

(i) For the (most common) case of turbulent flow, the (expensively calculated) turbulent diffusivity or viscosity is being used merely as a diagnostic to *switch off* its own effect in the governing equations. Results are virtually insensitive to the turbulence model used (except in boundary-layer regions).

(ii) Under the most favourable circumstances, one should expect that serious *quantitative* errors are being made. Profiles involving sharp changes in gradient are numerically smeared far beyond the correct physical diffusion rate. These solutions are only first-order accurate.

(iii) In some cases—for example, the thermally driven cavity flows described in this paper—the EDS-based solutions are not even *qualitatively* correct. Physically observed phenomena, such as recirculation cells, for example, are not captured—because the *effective* Péclet or Reynolds numbers are significantly too small.

Although EDS-based schemes *may* give plausible (and, in hindsight, even adequate) solutions under some circumstances, in a truly predictive situation these methods are simply too unreliable for practical use. Fortunately, in all flow regimes, modern cost-effective high-order methods, incorporating flux-limiters and deferred-correction techniques, not only give highly accurate physically responsive results, but they are also entirely compatible with traditional tridiagonal ADI solution strategies—requiring relatively minor coding modifications in the source terms of the iterative solver.

Exponential-based schemes such as Hybrid and Power-Law should be considered as being of historical interest in the evolution of CFD schemes. *They should not be used for practical*

calculations. There is one situation in which purely first-order convection (plus second-order diffusion) could be useful: debugging aspects of a *new* CFD-code—such as the grid generator or the graphics package. If the computation blows up or other problems arise, the difficulties are probably *not* with the mild-mannered convection–diffusion scheme. This is easily implemented: simply suppress the correction terms in the deferred-correction procedure. When the (non-convection–diffusion) problems are fixed, the higher-order flux-limited correction terms can be re-activated.

Finally, there is an exceedingly practical reason why Hybrid, Power-Law or related exponential schemes should not be used for convective modelling: *there is an increasing probability that the results will not be published in archival journals.* In recent years, there has been a considerable amount of 'behind-the-scenes' activity—in addition to open discussion[27]—on the question of numerical uncertainty. The basic philosophy is that a paper (or conference presentation) describing the results of a numerical simulation of a practical problem should at least *address* problems of numerical uncertainty, just as experimental papers routinely *assess* experimental uncertainty in their results. Journal editors and conference organizers are increasingly aware of the need for guidelines to be established, outlining criteria to be addressed. The ASME *Journal of Fluids Engineering* has taken the lead in this respect, based on the considerable efforts of the ASME Co-ordinating Group on Computational Fluid Dynamics.[28] Volume 115 of the *Journal of Fluids Engineering* (September 1993) describes in an editorial a 10-point list of criteria in both long and short forms. For example, items 2 and 3 state[29]

2. Methods must be at least second-order accurate in space.
3. Inherent or explicit artificial viscosity (or diffusivity) must be assessed and minimized.

More specifically, the expanded versions of items 2 and 3 state[29]

2. The numerical method used must be at least formally second-order accurate in space . . . it has been demonstrated many times that, for first-order methods, the effect of numerical diffusion on the solution is devastating.
3. Methods using a blending or switching strategy between first and second order methods (*in particular, the well-known 'hybrid,' 'power-law' and related exponential schemes*) will be viewed as first-order methods, unless it can be demonstrated that their inherent numerical diffusion does not swamp or replace important modelled diffusion terms . . . [emphasis added]

The *AIAA Journal* has also recently adopted a uniform policy on both experimental and numerical uncertainty analysis.[30] A number of other editorial boards are presently considering and implementing similar policies.[31]

ACKNOWLEDGEMENT

Portions of the first author's research has been supported by the Institute for Computational Mechanics in Propulsion at the NASA Lewis Research Center under Space Act Agreement NCC 3-233.

REFERENCES

1. D. N. deG. Allen and R. V. Southwell, 'Relaxation methods applied to determine the motion, in two dimensions, of a viscous fluid past a fixed cylinder', *Q. J. Mech. Appl. Maths.*, **8**, 129–145 (1955).
2. G. D. Raithby and G. E. Schneider, 'Elliptic systems: Finite-difference method II', in W. J. Minkowycz *et al.* (eds.), *Handbook of Numerical Heat Transfer*, Wiley, New York, 1988, pp. 241–294.

3. D. B. Spalding, 'A novel finite difference formulation for differential expressions involving both first and second derivatives', *Int. j. numer. methods eng.*, **4,** 551–559 (1972).
4. S. V. Patankar, *Numerical Heat Transfer and Fluid Flow*, Hemisphere, New York, 1980.
5. A. D. Gosman and W. M. Pun, 'Calculation of recirculating flows', *Heat Transfer Section Report HTS/74/2*, Department of Mechanical Engineering, Imperical College, London, 1974.
6. R. W. Lewis (ed.), *Numerical Methods in Thermal Problems, Vol. VIII*, Pineridge, Swansea, 1993.
7. C. A. J. Fletcher, *Computational Techniques for Fluid Dynamics, Vols. I and II*, Springer, Berlin, 1988.
8. R. M. Smith and A. G. Hutton, 'The numerical treatment of advection: a performance comparison of current methods', *Numer. Heat Trans.*, **5,** 439–461 (1982).
9. B. P. Leonard and S. Mokhtari, 'ULTRA-SHARP solution of the Smith–Hutton problem', *Int. J. Numer. Methods Heat Fluid Flow*, **2,** 407–427 (1992).
10. B. P. Leonard, 'Elliptic systems: Finite difference method IV', in W. J. Minkowycz *et al.* (eds.), *Handbook of Numerical Heat Transfer*, Wiley, New York, 1988, pp. 347–378.
11. B. P. Leonard and S. Mokhtari, 'Beyond first-order upwinding: the ULTRA-SHARP alternative for nonoscillatory steady-state simulation of convection', *Int. j. numer. methods eng.*, **30,** 729–766 (1990).
12. B. P. Leonard, 'A consistency check for estimating truncation error due to upstream differencing', *Appl. Math. Modelling*, **2,** 239–244 (1978).
13. C. M. Vest and V. Arpaci, 'Stability of natural convection in a vertical slot', *J. Fluid Mech.*, **36,** 1–15 (1969).
14. J. E. Drummond and S. A. Korpela, 'Natural convection in a shallow cavity', *J. Fluid Mech.*, **182,** 543–564 (1987).
15. J. E. Drummond, A. J. Yovichin and J. P. McKee, 'The effect of upwind formulations on secondary flows in a thermally-driven cavity', *Proc. of 3rd ASME-JSME Thermal Eng. Joint Conf.*, Vol. 1, ASME, New York 1991, pp. 47–54.
16. A. Arakawa, 'Computational design for long-term numerical integration of the equations of motion: two-dimensional incompressible flow, Part 1', *J. Comput. Phys.*, **1,** 119–143 (1966).
17. J. E. Fromm, 'A method for reducing dispersion in convective difference schemes', *J. Comput. Phys.*, **3,** 176–189 (1968).
18. B. P. Leonard, 'A stable and accurate convective modelling procedure based on quadratic upstream interpolation'. *Comput. Methods Appl. Mech. Eng.*, **19,** 59–98 (1979).
19. P. K. Khosla and S. G. Rubin, 'A diagonally dominant second-order accurate implicit scheme', *Comput. Fluids*, **2,** 207–218 (1974).
20. T. Hayase, J. A. C. Humphrey and R. Greif, 'A consistently formulated QUICK scheme for fast and stable convergence using finite-volume iterative calculation procedures', *J. Comput. Phys.*, **98,** 108–118 (1992).
21. F. S. Lien and M. A. Leschziner, 'Approximation of turbulence convection in complex flows with a TVD-MUSCL scheme', *Proc. 5th Int. IAHR Symp. on Refined Flow Modelling and Turbulence Measurements*, Paris, September 1993.
22. P. H. Gaskell and A. K. C. Lau, 'Curvature-compensated convective transport: SMART, a new boundeness preserving transport algorithm', *Int. j. numer. methods fluids*, **8,** 617–635 (1988).
23. B. P. Leonard, 'Simple high accuracy resolution program for convective modelling of discontinuities', *Int. j. numer. methods fluids*, **8,** 1291–1318 (1988).
24. P. K. Sweby, 'High resolution schemes using flux limiters for hyperbolic conservation laws', *SIAM J. Numer. Anal.*, **21,** 995–1011 (1984).
25. H. T. Huynh, 'Accurate monotone cubic interpolation', *SIAM J. Numer. Anal.*, **30,** 57–100 (1993).
26. S. Mokhtari, 'Development and analysis of steady high-resolution non-oscillatory convection schemes using higher-order upwinding', *Ph.D. Dissertation*, The University of Akron, Akron, OH, 1991.
27. I. Celik, 'Numerical uncertainty in fluid flow calculations: Needs for future research', ASME *J. Fluids Eng.*, **115,** 194–195 (1993).
28. I. Celik, C. J. Chen, P. J. Roache, and G. Scheuerer (eds.), *Quantification of Uncertainty in Computational Fluid Dynamics*, ASME FED–Vol. 158, New York, 1993.
29. C. J. Freitas, Editorial, ASME *J. Fluids Eng.*, **115,** 339–340 (1993).
30. Editorial, *AIAA J.*, **32,** 3 (1994).
31. Editorial, *Int. j. numer. methods fluids*, **19**(7), iii (1995).